Expanded View Figures

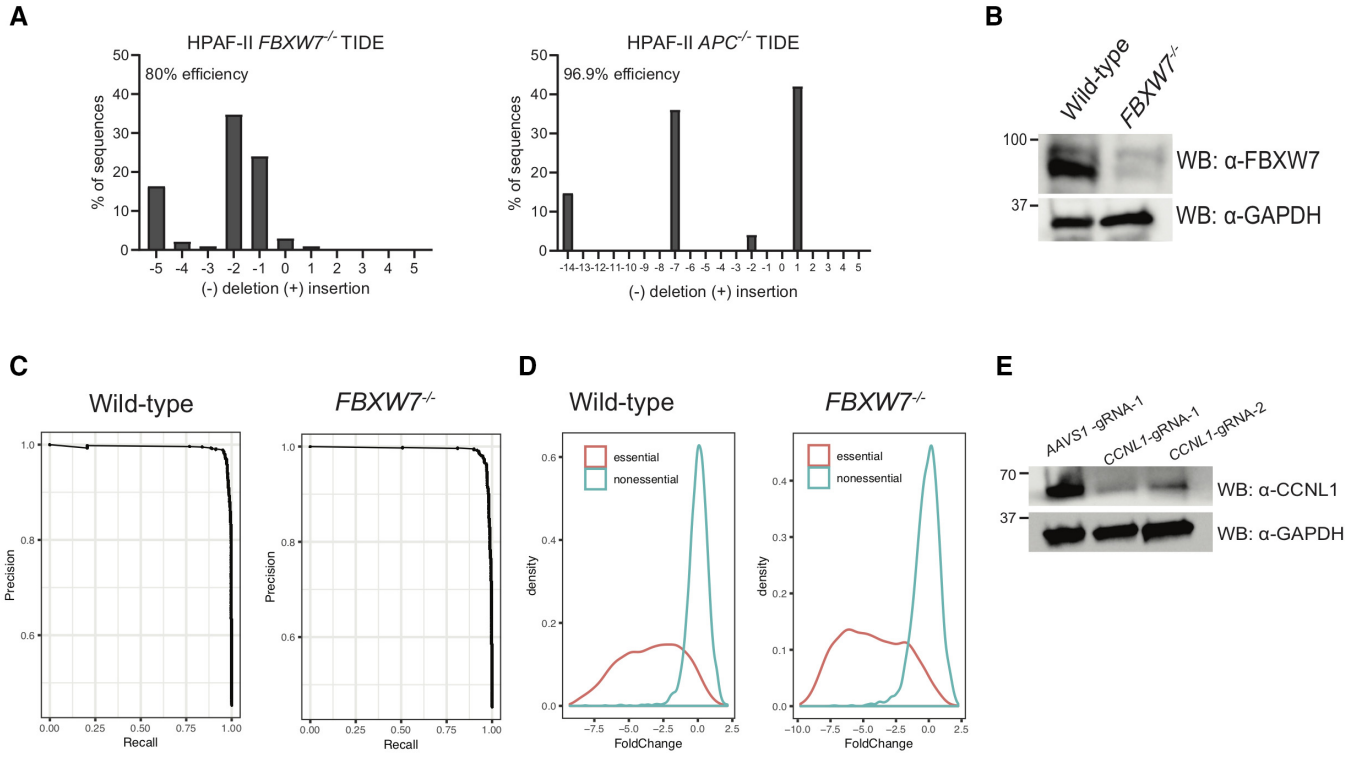

Figure EV1. Verification of *FBXW7* and *APC* knockout & genome-wide screen quality control.

A TIDE analysis of HPAF-II *FBXW7*$^{-/-}$ cell line and HPAF-II *APC*$^{-/-}$ cell line.

B Immunoblot of lysates extracted from HPAF-II *FBXW7*$^{-/-}$ cell lines demonstrating knockout of FBXW7 protein expression.

C Fold-change plots of HPAF-II wild-type and *FBXW7*$^{-/-}$ genome-wide screens demonstrating a change in essential genes at T24 of the screen.

D Precision-recall curves of HPAF-II wild-type and *FBXW7*$^{-/-}$ genome-wide screens demonstrating training sets of essential and nonessential genes performed appropriately in the BAGEL algorithm.

E Immunoblot of lysates extracted from *FBXW7*$^{-/-}$ cells following treatment with gRNAs targeting *CCNL1*.

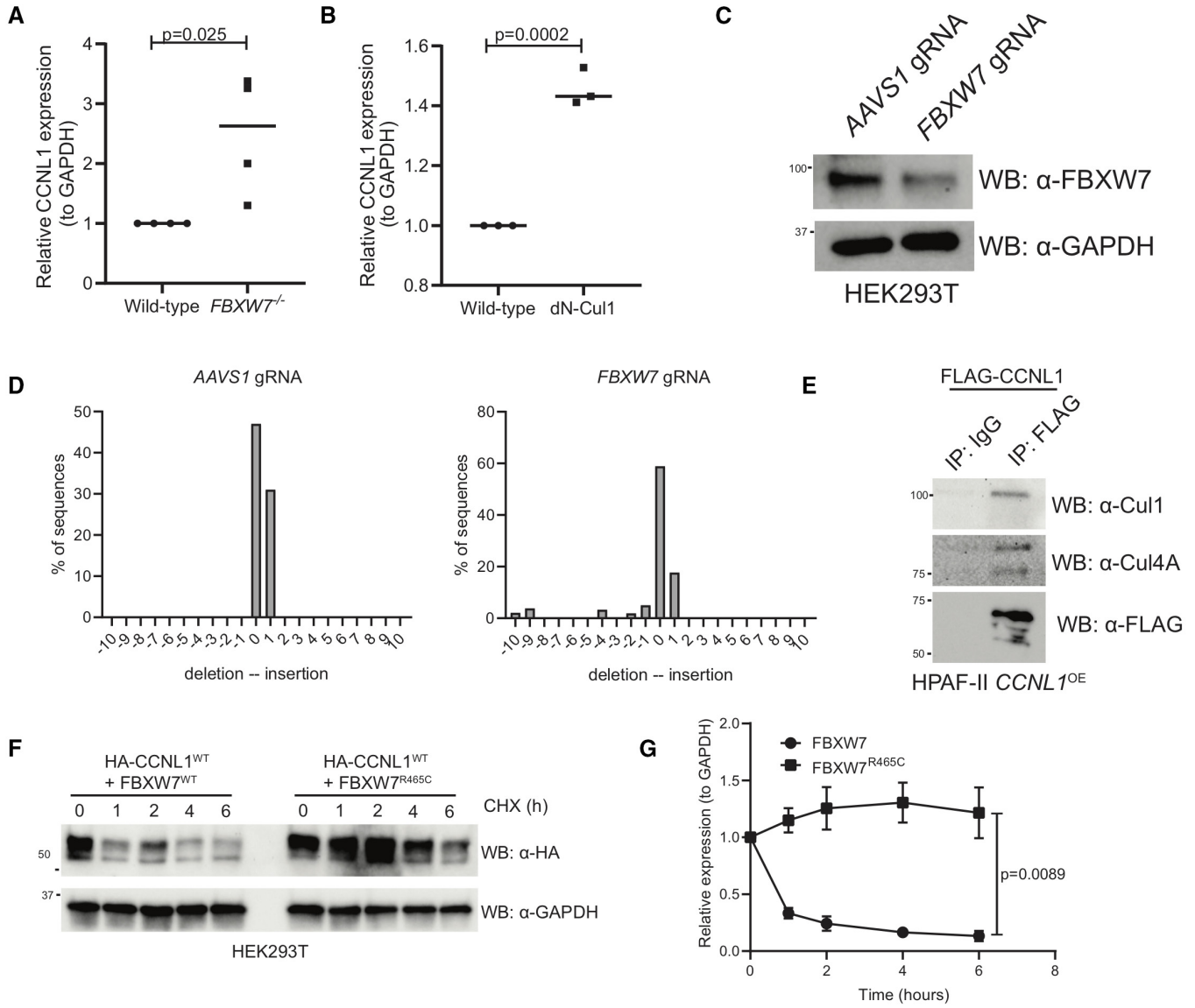

Figure EV2. CCNL1 degradation requires Cul1 and is blocked when substrate-binding deficient FBXW7^{R465C} is co-expressed.

A Quantification of immunoblots in Fig 3A, mean ± SEM, students *t*-test, $n = 3$ independent biological replicates.
B Quantification of immunoblots in Fig 3D, mean ± SEM, students *t*-test, $n = 3$ independent biological replicates.
C Immunoblot analysis of HEK293T cells expressing gRNAs against *AAVS1* or *FBXW7*.
D TIDE analysis of HEK293T cells expressing gRNAs against *AAVS1* or *FBXW7*.
E Immunoblot of immunoprecipitation of FLAG-CCNL1 overexpressed in HPAF-II cells, detecting endogenous Cul1 and Cul4A. Representative image of three independent replicates.
F Immunoblot of lysates following cycloheximide treatment of HEK293T cells expressing HA-CCNL1 and FLAG-FBXW7 or FLAG-FBXW7^{R465C}. Representative blot of three independent replicates.
G Quantification of cycloheximide chase in (F), mean ± SEM of three independent replicates, *t*-test at T6.

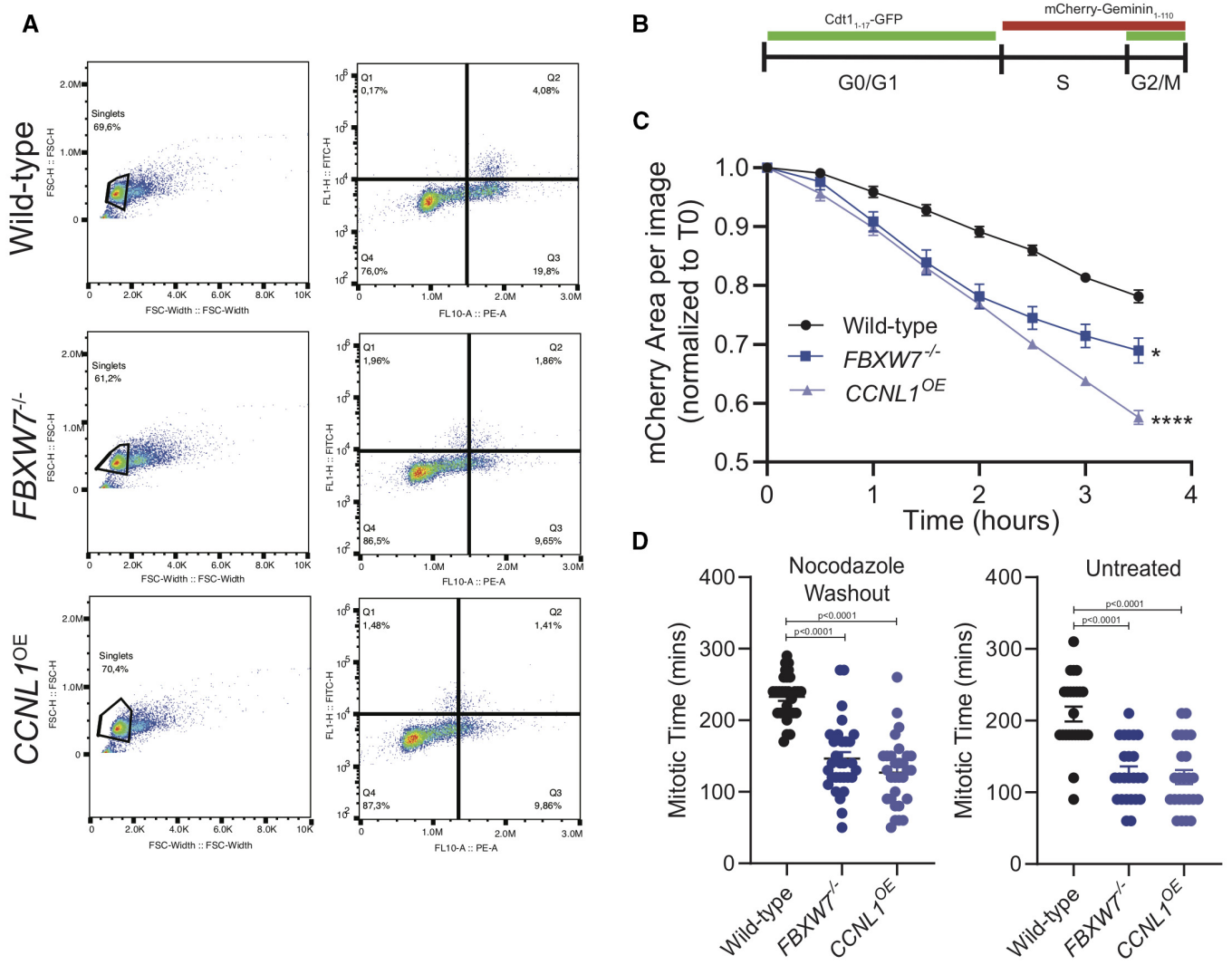

Figure EV3. HPAF-II FBXW7$^{-/-}$ and CCNL1^{OE} cells exit mitosis faster than wild-type.

A Representative images of gating strategy for HPAF-II wild-type, *FBXW7*$^{-/-}$ and *CCNL1*^{OE} cells to determine cell cycle distribution.

B Schematic of PIP-FUCCI reporter marker expression through three major cell cycle phases.

C Live-cell imaging of HPAF-II wild-type, *FBXW7*$^{-/-}$ and *CCNL1*^{OE} cells expressing PIP-FUCCI reporter treated with nocodazole overnight and released. Images collected over 3.5 h. Reduction in total population mCherry expression imaged over time, quantified in the Incucyte. Three independent replicates, mean ± SEM, two-way ANOVA, *$P = 0.0258$, ****$P < 0.0001$.

D Live-cell imaging of HPAF-II wild-type, *FBXW7*$^{-/-}$ and *CCNL1*^{OE} cells expressing PIP-FUCCI reporter either untreated or treated with nocodazole overnight and released. Measurement of individual cells as they lose mCherry expression. $n = 15$ cells per replicate, three independent replicates, one-way ANOVA, mean ± SEM.

Figure EV4. Genome-wide chemogenomic screen identifies CCNL1 and CDK11 are targets of OTS964.

A Representative gating strategy for HPAF-II wild-type, *FBXW7*$^{-/-}$ and *APC*$^{-/-}$ cells, with and without LGK974 treatment, to determine cell cycle distribution.

B Representative gating strategy for HPAF-II wild-type, *FBXW7*$^{-/-}$ and *CCNL1*^{OE} cells, with and without OTS964 treatment, to determine cell cycle distribution.

C Representative images of gating strategy for C33A, Caski, and SiHa cells, with and without OTS964 treatment, to determine cell cycle distribution.

D Normalized *Z*-score calculated in DrugZ plotted against gene rank for C33A chemogenomic screen with OTS964. Negative score indicates gene knockout synergistic with OTS964; positive score indicates gene knockouts resistant to OTS964. Red line marks the cutoff of FDR < 0.05.

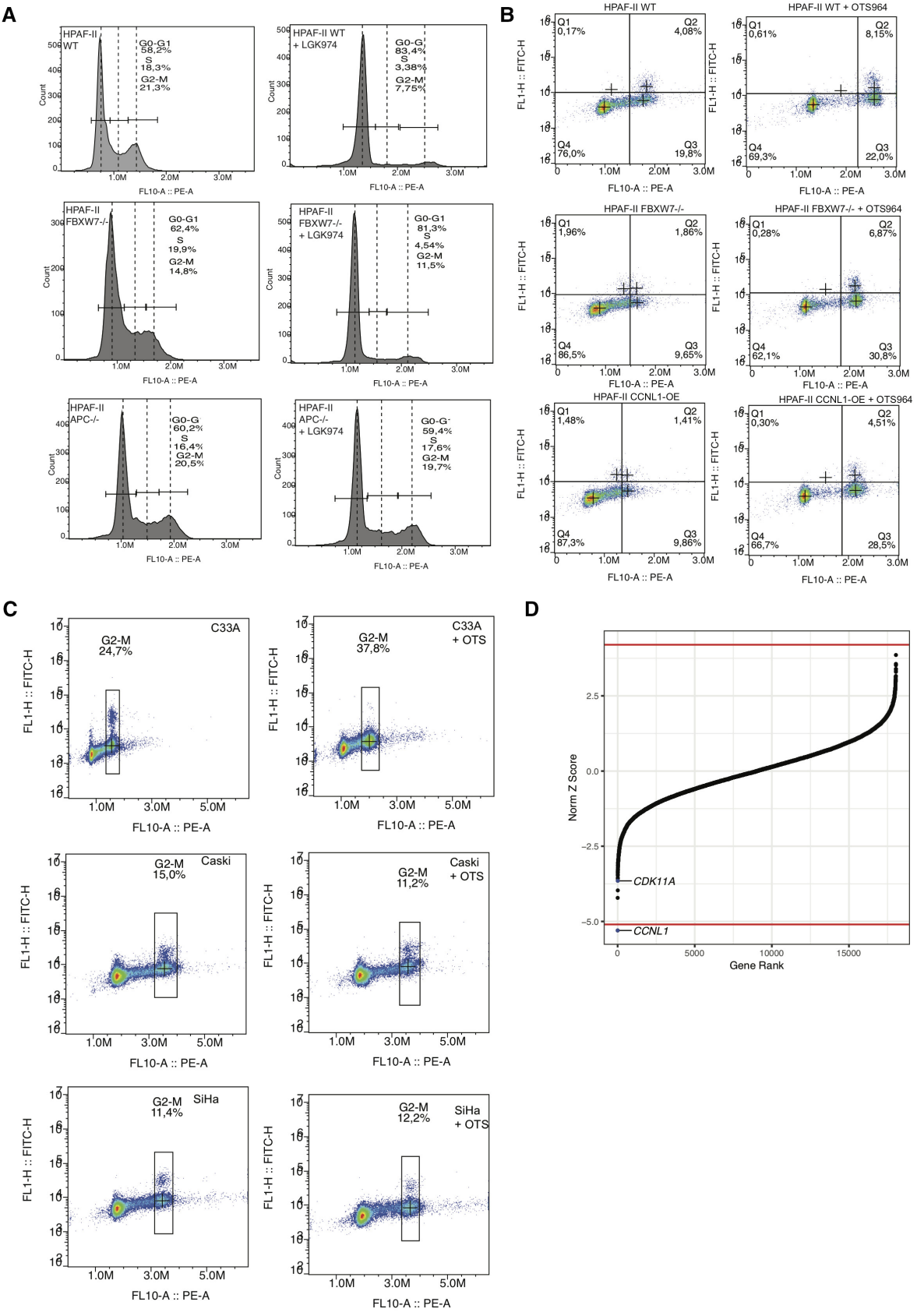

Figure EV4.